



Toward the ferroelectric field-effect transistor on BaTiO₃/LaMnO₃ heterostructure: DFT investigation

Irina Piyanzina^{1,2,*}  and Rinat Mamin^{1,2}

¹Zavoisky Physical-Technical Institute, FRC KazSC of RAS, Sibirskii trakt str. 10/7, Kazan, Russia 420029

²Institute of Physics, Kazan Federal University, Kremlyovskaya str. 16 a, Kazan, Russia 420008

Received: 2 September 2022

Accepted: 19 November 2022

© The Author(s), under exclusive licence to Springer Science+Business Media, LLC, part of Springer Nature 2022

ABSTRACT

We investigated the possibilities of switchable two-dimensional electron gas (2DEG) at the interface of antiferromagnetic and ferroelectric perovskites, LaMnO₃/BaTiO₃ (LMO/BTO) superlattice, by means of *ab initio* calculations. We show that in the LMO/BTO heterostructure the two-dimensional conducting state may be induced by applying external electrical field. Defects in the form of oxygen vacancies on the surface stimulate that phenomenon. The density of states at the Fermi-level can be tuned by ferroelectric polarization reversal. The conducting state is mainly localized within the interfacial MnO layer and it coexists with magnetic state, which arises mainly from Mn atoms.

Introduction

The ferroelectric films were already used in modern complementary metal-oxide semiconductor and other microelectronics processes as a gate material. It is therefore appealing to use ferroelectric materials in nonvolatile memory devices, such as ferroelectric random access memory (FeRAM) or ferroelectric field-effect transistors (FeFET). The presence of ferroelectric as a component of heterostructure gives us new outstanding functionality which can be used in possible electronic devices based on it. In particular, thanks to the presence of spontaneous polarization in the ferroelectric thin film, the two-dimensional gas (2DEG) [1] can occur at the interface. The electronic

properties of arising state can be tuned by an external field through the ferroelectric dipoles direction change. Investigations of heterostructures made it possible to combine incompatible mutually exclusive properties in one material, for instance, superconductivity [2–4] and magnetism [5] at the LaAlO₃/SrTiO₃ interface.

Most previous works on 2DEG at oxide interfaces were based mainly on SrTiO₃, in which the interfacial magnetism is very weak since of the nonmagnetic nature of their parent material. It was also shown that magnetism in such systems is induced by defects [6–11]. For instance, maximal magnetic moment induced by oxygen vacancy at the interface equals 0.2 μB per Ti atoms neighboring to the

Handling Editor: Till Froemling.

Address correspondence to E-mail: i.piyanzina@gmail.com

E-mail Address: rf_mamin@yahoo.com

<https://doi.org/10.1007/s10853-022-08000-2>

Published online: 30 November 2022

defect [12]. In such heterostructure the 2DEG arises due to the polar properties of LaAlO_3 . In contrast, the spontaneous electrical polarization of ferroelectric films, for instance BaTiO_3 , perpendicular to the interface can cause the accumulation of electrons in the interface area, and stimulate new non-trivial effects [13–15].

Despite a great interest to conducting heterostructures during last two decades and a huge number of research, this field is still fascinating and draws the attention discovering new phenomena [13–28]. To enhance interfacial magnetism, it is essential to use magnetic insulators as a component of heterostructures to support spin-polarized 2DEG. Even more promising here is the manipulation of its conducting state with the help of an electric field using ferroelectric materials [19–21]. Additional interest to such a heterostructures is associated with the possibility of controlling the ferromagnetic ordering at the interface due to interactions of spins through conduction electrons and with arising of multiferroic properties of all heterostructure. Multiferroic materials are compounds where at least two order parameters coexist in the same phase. One very important but extremely rare group is ferroelectric ferromagnets, which have recently stimulated an increasing number of research activities for their scientific uniqueness and application in the novel multifunctional devices [29–31]. Magnetoelectric materials are mainly interesting due to the possibility to control magnetic properties by an external electric field [32, 33]. Due to the extraordinary challenge of creating multiferroic compounds, it was essential to create superlattice multicomponent materials as more efficient. Moreover, the discovery of a quasi-two-dimensional electron gas properties in $\text{LaAlO}_3/\text{SrTiO}_3$ heterostructures has stimulated intense research activity in the last twenty years and provided new functionality for electronic devices [1, 2]. At the case of heterostructures we will have multiferroic material with spatially distributed properties. And thus, a converse magnetoelectric (ME) effect is realized, when magnetization can be changed by an electric field. For the purpose of ME coupling a great amount of various heterostructures have been investigated, most of which contain BaTiO_3 as a component such as Fe/BaTiO_3 [22], $\text{Co}_2\text{MnSi}/\text{BaTiO}_3$ [23], $\text{Fe}_3\text{O}_4/\text{BaTiO}_3$ [24], $\text{Fe}(\text{Ni}, \text{Co}, \text{CrO}_2)/\text{BaTiO}_3/\text{normal metal}$ [25], $\text{La}_{1-x}\text{A}_x\text{MnO}_3/\text{BaTiO}_3$ ($\text{A} = \text{Ba}, \text{Sr}, \text{and Ca}$) [13], $\text{LaMnO}_3/\text{BaTiO}_3/\text{SrMnO}_3$ [26], $\text{La}_{1-x}\text{Sr}_x$

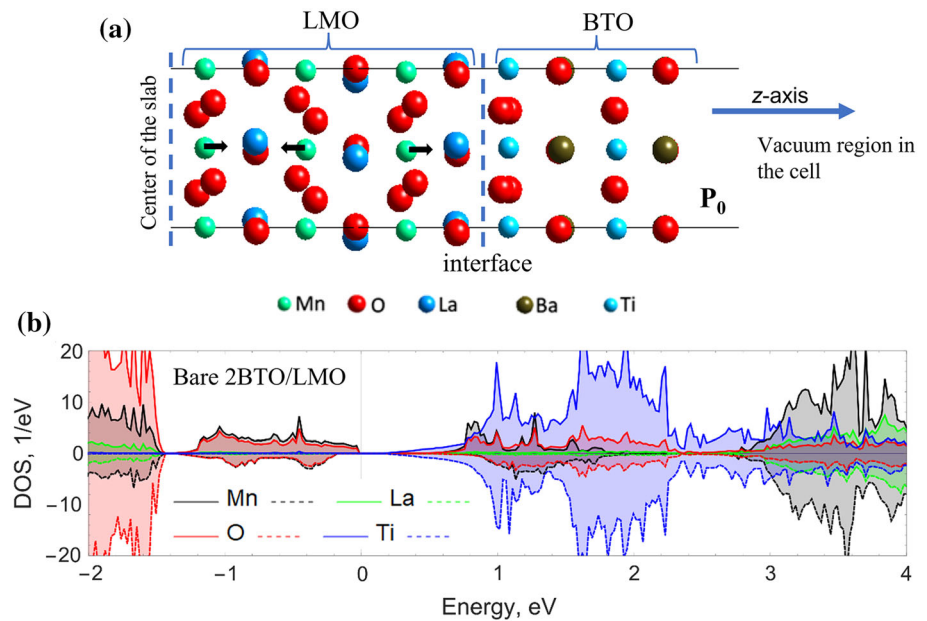
$\text{MnO}_3/\text{BaTiO}_3$ [27]. The possibility to control both conductivity and magnetism by an electric field in the interface of heterostructures in the $\text{BaTiO}_3/\text{LaMnO}_3$ was discussed recently in Ref. [34, 35]. More recently the spin-dependent switching effect was demonstrated on a similar system based on perovskites $\text{YTiO}_3/\text{PbTiO}_3$, where antiferromagnet (AFM) YTiO_3 was used as a source of magnetism, and ferroelectric (FE) PbTiO_3 was used to manipulate the interfacial states [28]. The use of A-type AFM material was supported by the fact that the A-type AFM order is better coupled with the field effect, since the FE field effect and the A-type AFM order are layer dependent.

When 2DEG occurs, the issue of switching such states by external influence is acute. To achieve this goal, in the present work, the $\text{LaMnO}_3/\text{BaTiO}_3$ (LMO/BTO) heterostructure along the [001] direction is studied as a model system. Based on density functional theory (DFT) calculations, we investigate the possibilities of the spin-polarized 2DEG appearing in the LMO/BTO heterostructure. In particular, the essential issue is understanding the influence of polarization inside the BTO slab on the interfacial electronic states. To do this, we compare the electronic properties of the BTO/LMO heterostructure with the same heterostructure with a simulated additional polarization. We consider two cases: polarization directed toward the interface (P_{down}) and the surface (P_{up}). Finally, the impact of oxygen vacancies located on the surface on the electronic and magnetic properties is analyzed.

Methodology

The present research were performed by using the *ab initio* calculations as based on density functional theory (DFT) [36, 37] as implemented in the Vienna Ab-Initio Simulation Package (VASP) [38–40], which is part of the Medea[®] software of Materials Design [41]. All computational parameters and supercells are in consistence with our previous researches [35, 42], where an impact of ferroelectric thickness onto the electronic states was analyzed. Here, the polarization direction was changed in the LMO/BTO heterostructure with 2 BTO overlayers, the right half of the fully optimized unit supercell is presented in Fig. 1.

Figure 1 **a** Right half structures of the LMO/2BTO supercell. The dashed line corresponds to the middle of the slab, whereas the second half is a mirror copy. A vacuum region of ~ 20 Å was added, which is not shown here. The cell configuration is in consistency with Ref. [42]. P_0 denotes the polarization appearing in the system. **b** The corresponding atom-resolved density of states spectrum.



We have checked the influence of different computation and geometry parameters: the size of the cell, thickness of ferroelectric layer, thickness of LMO substrate, termination types. Obvious, more accurate calculations would change the numbers, but here, we used a big supercell with 114 atoms, so we used highest possible accuracy within the reasonable computation time. The cell parameters a and b were chosen to be the same as the optimized bulk LMO cell parameters reflecting the substrate conditions. Besides, we checked slightly bigger cell parameters and got that the properties of interest do not change. The c parameter was chosen to be big enough in order to prevent the interaction between periodic copies, all the atoms were allowed to relax in z -direction. The size of ferroelectric film thickness has been investigated in our previous research [42]. There, we have obtained that system remains a semiconductor up to 6 BTO overlayers. The band gap decreases with increasing the thickness and system most probably becomes a conductor with sufficient thickness, but that does not affect quantitative conclusions made in the current paper. Concerning LMO thickness and terminations we found that the stable heterostructures exist only with a particular LMO termination. The supercell used here consists of 11 alternating layers and MnO_2 terminating layers. Another termination was found to be not stable. The less layered heterostructures are too thin to make any conclusion, and more layers require significant

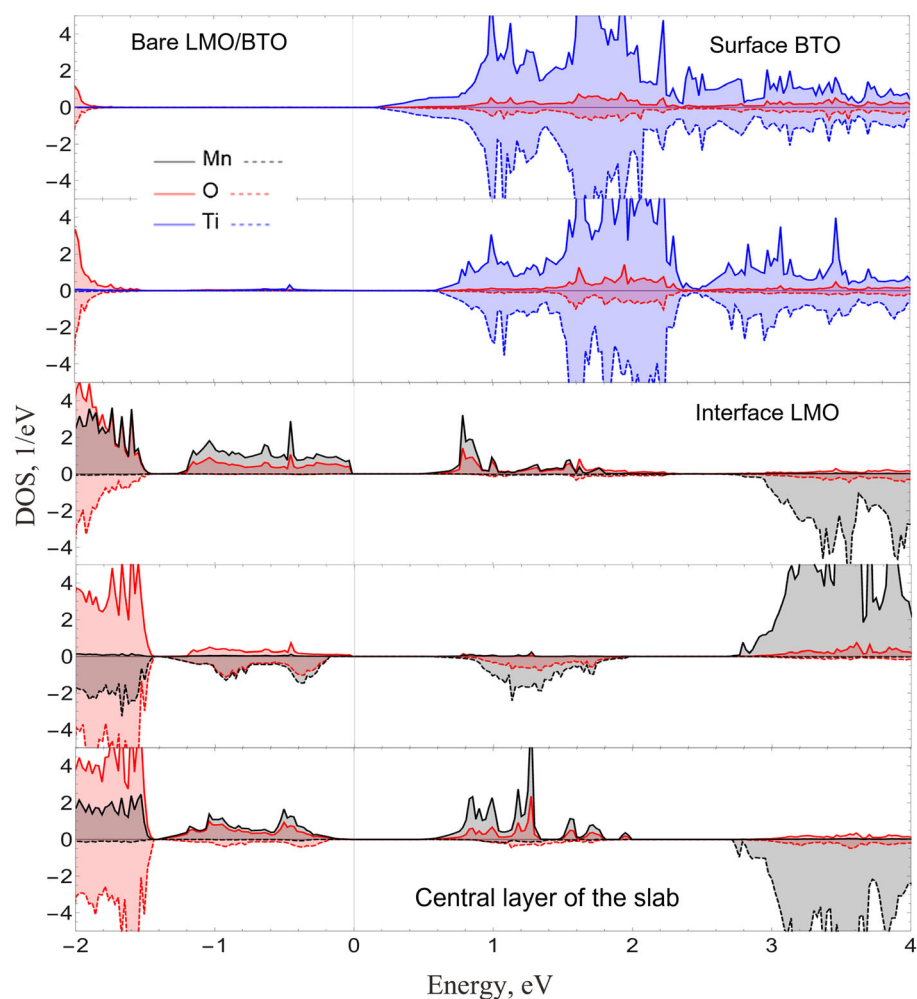
computational resources we do not possess, unfortunately. However, we could assume, that the thickness of LMO does not significantly affect the overall electronic properties since the properties of interest mostly depend on the external ferroelectric overlayers.

Results and discussion

In the beginning, we have checked the parent materials of the heterointerface separately in the bulk and thin-film geometries to ensure the reproducibility of the results obtained by the method and calculation parameters used. Those results are listed in our resent research [42]. There we confirmed that both materials in bulk and thin film geometries remain insulating, BTO is non-magnetic, LMO was chosen to be in the A-AFM ordering in accordance with previous research, where it was suggested to replace ferromagnetic material by antiferromagnetic to realize the spin-dependent switching effect [28, 35]. BaTiO_3 is a well-known ferroelectric, which has a ferroelectric spontaneous polarization based on the shift of the Ti atom in the O_6 octahedra in different directions depending on the phase.

An important note here concerning the choice of BTO ferroelectric phase. Barium titanate (BTO) crystals exhibit phase transitions from the cubic paraelectric phase Pm-3m to the tetragonal ferroelectric phase P4mm at about 403 K, then to the

Figure 2 The layer and atom-resolved density of states spectra of the LMO/BTO heterostructure with two BTO overlayers. Note that the spectra are shown only for half slab, whereas the other half has the same spectra.



orthorhombic $Amm2$ phase at about 278 K, and to the rhombohedral $R3m$ phase at about 183 K [43]. Therefore, below 170 K, the stable structure of BTO single crystals is rhombohedral. And this is true for bulk samples only. In the case of films, the picture changes radically. Films of BTO and its solid compositions of the $Ba_{0.8}Sr_{0.2}TiO_3$ (BST) type, depending on the magnitude and sign of deformation, experience ferroelectric phase transitions from the cubic phase to the tetragonal phase with polarization perpendicular to the substrate, or to the orthorhombic phase with polarization parallel to the substrate (see for example $Ba_{0.8}Sr_{0.2}TiO_3$ (BST) films on (001) MgO substrates [44]). In the case of BTO on LMO, in the configuration when the axis with LMO is perpendicular to the surface (this is the case we are considering), a sufficiently significant compressing deformation arises, which “supports” the tetragonal

phase. This compressing strain causes the unit cell to shrink in the a and b directions, and therefore “elongate” in the c direction, which effectively stimulates the phase transition to the ferroelectric state. In this case, firstly, the tetragonal phase appears at much higher temperatures (for example, for BST films on (001) MgO substrates T_c 540 K), and secondly, the tetragonal phase remains stable up to the lowest temperatures. Our preliminary studies of BST films on (001) LMO substrates have shown that the tetragonal phase is stable from room temperature to at least liquid nitrogen temperature (~ 77.4 K). Therefore, we assume that tetragonal phase in the thin film BTO might conserve up to 0 K.

In order to merge BTO with LMO with polarization of BTO being parallel to the c -axis of LMO, the BTO unit cell has to be rotated by 45° along z -axis. In this geometry the $a_{BTO} \times \sqrt{2}$ is very close to the a_{LMO} and

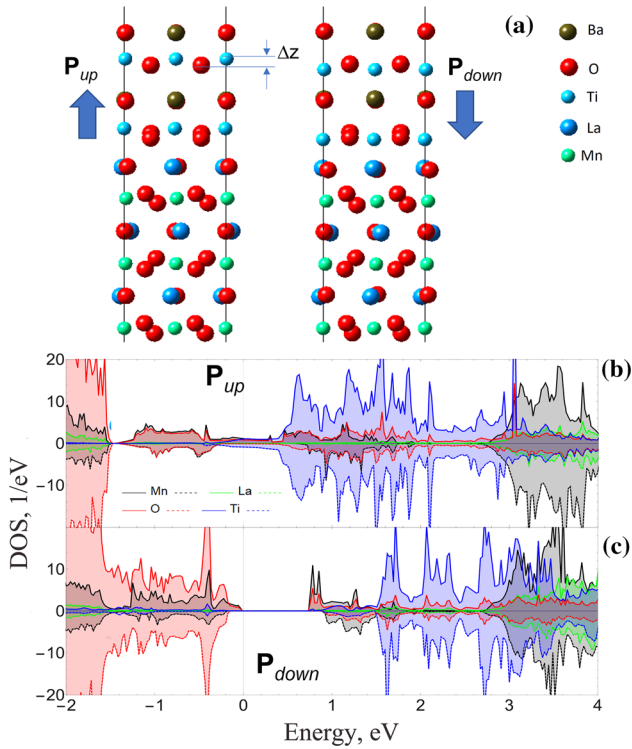


Figure 3 a Upper half structures of LMO/BTO supercells with simulated imposed polarization, i.e., dipoles directed toward the surface (P_{up}) and toward the interface (P_{down}), as indicated by blue arrows. Corresponding density of states spectra for two polarization directions P_{up} (b) and P_{down} (c). The same atoms designation was used as shown in Fig. 1.

b_{LMO} cell parameters. The resulted supercell with two BTO overlayers is presented in Fig. 1a, where the right half of the unit cell is presented without presenting the full vacuum region. The structure was fully optimized.

Performed structural optimization resulted in a slight displacement of Ti atoms out of oxygen planes. Except for the one, all Ti atoms shift toward the surface. As a result the total polarization is directed predominantly toward the surface. We denote that polarization as P_0 . Such a structural reconstruction leads to an electronic rearrangement as reflected in the atom-resolved DOS (Fig. 1b). A larger number of BTO overlayers was checked as well, and we got that, quantitatively, all heterostructures with up to 6 BTO overlayers represent similar DOS, but with decreasing band gaps as reflected in Ref. [42]. The layer-resolved DOS spectrum for the bare LMO/BTO heterostructure with 2 BTO overlayers is shown in Fig. 2 for further comparison.

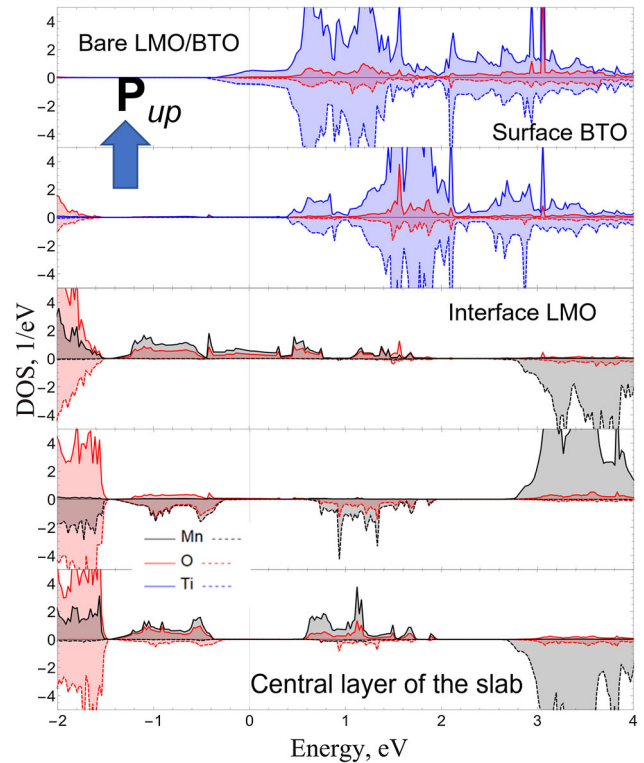
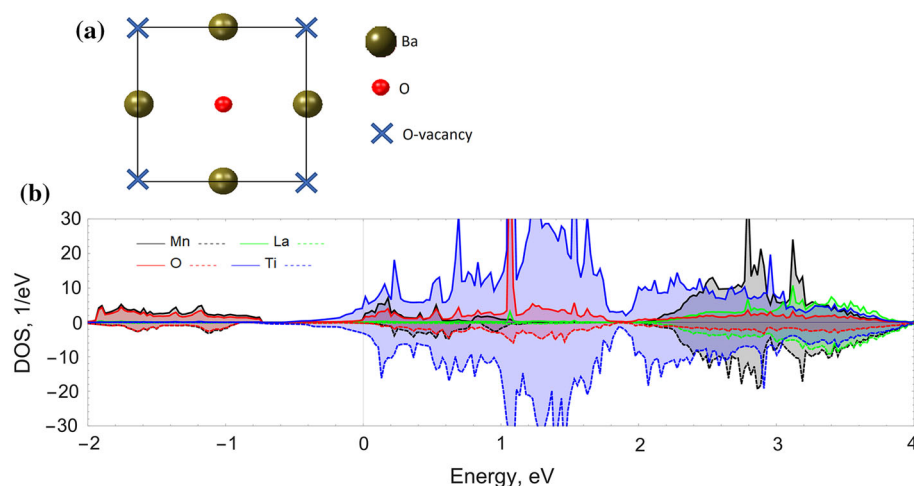


Figure 4 The layer-resolved density of states spectra for the LMO/BTO heterostructure with polarization directed toward the surface. Note that the spectra are shown only for the half slab, whereas the other half has the same spectra.

Polarization impact

To simulate the application of an external electric field and, as consequence, the occurrence of additional polarization in the positive or negative directions with respect to the z -axis we chose the LMO/BTO heterostructure with two BTO overlayers. There, all Ti atoms were moved out of the oxygen planes up or down by $\Delta z_{Ti-O} \sim 0.2 \text{ \AA}$ with respect to the position found in full optimization, and the TiO_2 layers within the BTO slabs were kept frozen during the optimization, whereas the central atoms of LMO were all fully relaxed. This shift value was chosen close to the Ti shift due to spontaneous ferroelectric polarization in the bulk tetragonal BTO. The two considered supercells are shown in Fig. 3a with corresponding DOS (b is for polarization directed toward the surface (P_{up}) and c-directed toward the interface (P_{down})). It is clearly observed from DOS plots that polarization direction affects the electronic properties of the considered LMO/BTO heterostructure. In particular, polarization toward the surface of

Figure 5 **a** Top view onto the surface BaO layer of LMO/BTO heterostructure with three BTO overlayers and one oxygen vacancy **(b)** and corresponding atom-resolved density of states.



the heterostructure reduces the band gap and leads to a semiconductor–conductor transition, whereas the second case of polarization directed toward the interface increases the band gap from 0.25 up to 0.31 eV.

At the next step, magnetic states have been examined, and we found that the distribution of magnetic moments within the MnO layers does not change significantly. However, the total magnetization is the lowest for P_{down} and the highest for P_0 . So, the magnetoelectric coupling takes place, but as not as pure as in Ref. [28] for $\text{YTiO}_3/\text{PbTiO}_3$, where the interfacial magnetic moments turn to zero for P_{up} . The possible reason could well be the usage of different supercells, in particular, in the mentioned research, there is even number of MnO layers and, consequently, the pure A-AFM ordering in the YTiO_3 slab. In contrast, in our case the total magnetization is not zero due to presence of the even number of MnO_2 layers. Besides, the slab is not symmetrical, and no vacuum was added in contrast to our supercell. Similar system was also investigated previously by Ciucivara et al. [34], where $(\text{LaMnO}_3)_{4.5}/(\text{BaTiO}_3)_{4.5}$ superlattice was considered with the vacuum region. They reported that starting with A-AFM LaMnO_3 the optimization of the superlattice converged to the ferromagnetic order. The study concluded that interfaces increase the magnetization and may favor ferromagnetic ordering.

Finally, for a conducting heterostructure with polarization toward the surface (P_{up}) we present the layer-resolved DOS (shown in Fig. 4). It reveals that the Fermi-level is mainly crossed by states filled with

electrons of interfacial Mn atoms of LMO, implying an interfacial 2DEG. The DOS at the Fermi level for the second and third layers inside the LMO slab are equal to zero. Compared to the case without additional polarization (P_0) demonstrated above (Fig. 2), polarization toward the surface leads to a downshift of the Ti states in the ferroelectric slab. As a consequence, that leads to the surface conductivity, and, more importantly, to the interfacial conductivity with Mn 3d contribution. The mechanism of the appearance of conductivity might well be as follows: the ferroelectric polarization toward the surface of the slab leads to the electric field strength being directed from LMO to the surface of the BTO. Therefore, all electrons will be attracted by the lowest interfacial layer and confined close to the interface.

Oxygen vacancies impact

To check other possibilities for conducting state creation the oxygen vacancies were created at the surface layers of the slab of the LMO/BTO heterostructure with 3 BTO overlayers. Oxygen vacancies were introduced on both sides while preserving the inversion symmetry of the slabs. The top view of the surface layer and corresponding atom-resolved DOS for the LMO/BTO heterostructure with a vacancy in the surface layer is presented in Fig. 5a.

Depicted situation results in a Ba_2O surface layer with a formal charge +2 and occupation of the lowest part of the conduction band, which is of Ti, Mn 3d and O 2p characters as shown in DOS (Fig. 5b). For this configuration, the layer-resolved DOS was

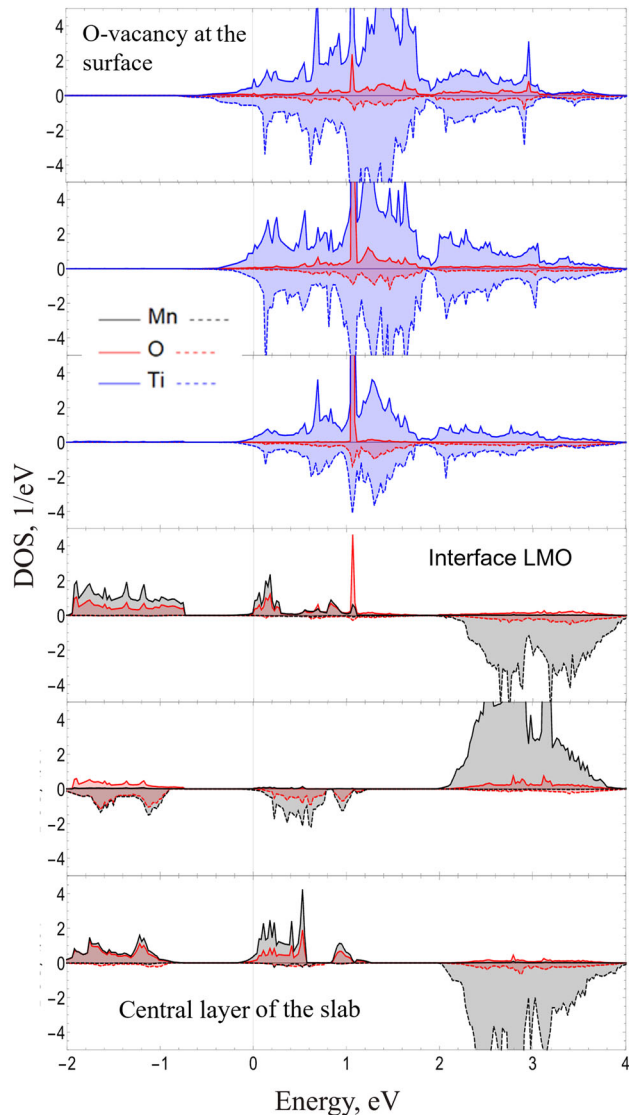


Figure 6 The layer-resolved density of states spectra for the LMO/BTO heterostructure with one oxygen vacancy per the 1×1 surface. Note that the spectra are shown only for the half slab, whereas the other half has the same spectra.

calculated as well (Fig. 6). Since a positive charge is created on the surface, the occurrence of the conducting state on the surface is not surprising. Besides, the charge reconstruction takes place leading to the downshift of Mn and O states in the LMO slab and crossing the Fermi-level. Therefore, the situation with vacancies is similar to the case of applying an electrical field toward the surface, which was discussed in the previous section.

Discussion

In the bare LMO/BTO heterostructure (Fig. 7a), the structural optimization resulted in the shift of Ti atoms out of the oxygen planes toward the surface of the slab. This shift corresponds to the polarization and, hence, to the electrical field directed toward the surface (as denoted by arrows). Such a structural reconstruction leads to an electronic reconstruction and corresponding downshift of the states located above the Fermi-level, to the closing of the band gap with more than 6 ferroelectric layers [42]. The distribution of charges during arising the electrical field toward the surface is shown in (Fig. 7a), in particular, electrons move against the field to the interface, and holes—with the field to the surface of the slab. Similarly, if additional polarization takes place (Fig. 7b), the number of charges increases and a significant contribution arises at the interface. This is also seen in the layer-resolved DOS spectra (Figs. 2 and 4), where the Mn interface and Ti surface states cross the Fermi-level. On the contrary, the situation in Fig. 7c with polarization directed toward the interface leads to the counter motion of charges and opposite motion of electronic states upward (Fig. 3b). In this case, the number of holes at the interface is small because a higher value of electrical field is required in order to move more charges and move electronic states higher in order to contribute significantly to the Fermi-level. The last considered here case of heterostructure with oxygen vacancy on the surface (Fig. 7d) is similar to the case with upward directed polarization (Fig. 7b). Here, the presence of a vacancy leads to the appearance of an extra positive charge on the surface. Therefore, this increases the electrical field through the ferroelectric film and the flow of electrons down to the interface and holes up to the surface (this is also seen in the layer-resolved DOS (Fig. 6).

Summary

In summary, by means of *ab initio* calculations, we have demonstrated that the combination of FE polarization and antiferromagnetism at the interface can affect the electronic and magnetic properties. In particular, the additional polarization imposed by the external electric field directed toward the surface of the LMO/BTO heterostructure with two BTO overlayers can change the conducting state from

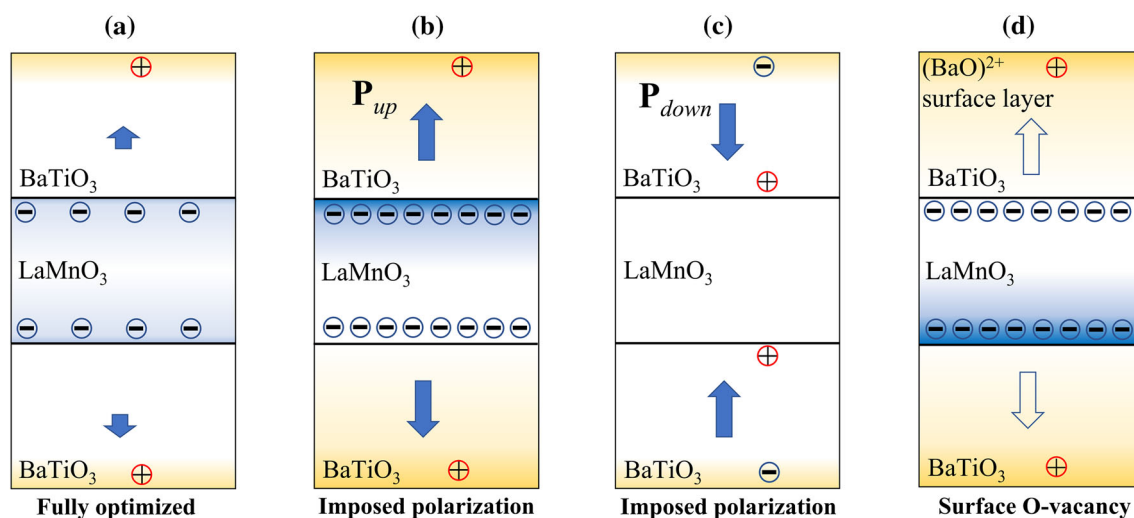


Figure 7 A schematic of the effect of polarization direction and oxygen vacancy on the conductivity of a ferroelectric/antiferromagnet heterostructure. **a** For an optimized heterostructure, the intrinsic polarization is directed toward the surfaces. The majority of charge is redistributed by the electrostatic field. Electrons and holes are mainly located near the interface and surface layers, respectively. **b** When the polarization is enhanced

semiconductor to a conductor due to the additional polarization. Similarly, oxygen vacancies located on the surface of a ferroelectric film can change the charges distribution in the slab, which leads to a downshift of the Mn and O states in the LMO slab and appearance of nonzero DOS at the Fermi-level and, as a consequence, conductivity with an interface contribution.

Acknowledgments

Computing resources were provided by the Laboratory of Computer design of new materials at Kazan Federal University.

Funding

The reported study was funded by the Russian Scientific Foundation according to research Project No. 21-12-00179.

by an external field, the carrier density mainly at the interface increases. **c** When the polarization direction is reversed, the majority charge carriers are pushed away from the interface, reducing the conductivity and switching the system to the off state. **d** Similar to the (**b**) case, a surface vacancy results in a positively charged surface and consequent polarization directed toward the surface and an increase in the density of states at the Fermi-level.

References

- [1] Ohtomo A, Hwang HY (2004) A high-mobility electron gas at the $\text{LaAlO}_3/\text{SrTiO}_3$ heterointerface. *Nature* 427(6973):423–426. <https://doi.org/10.1038/nature02308>
- [2] Reyren N, Thiel S, Cavaglia AD, Kourkoutis LF, Hammerl G, Richter C, Schneider CW, Kopp T, Rüetschi AS, Jaccard D, Gabay M (2007) Superconducting interfaces between insulating oxides. *Science* 317(5842):1196–1199. <https://doi.org/10.1126/science.1146006>
- [3] Bert JA, Kalisky B, Bell C, Kim M, Hikita Y, Hwang HY, Moler KA (2011) Direct imaging of the coexistence of ferromagnetism and superconductivity at the $\text{LaAlO}_3/\text{SrTiO}_3$ interface. *Nat Phys* 7(10):767–771. <https://doi.org/10.1038/nphys2079>
- [4] Li L, Richter C, Mannhart J, Ashoori RC (2011) Coexistence of magnetic order and two-dimensional superconductivity at $\text{LaAlO}_3/\text{SrTiO}_3$ interfaces. *Nat Phys* 7(10):762–766. <https://doi.org/10.1038/nphys2080>
- [5] Brinkman A, Huijben M, Van Zalk M, Huijben J, Zeitler U, Maan JC, van der Wiel WG, Blank DH, Rijnder G, Hilgenkamp H (2007) Magnetic effects at the interface between non-magnetic oxides. *Nat Mater* 6(7):493–496. <https://doi.org/10.1038/nmat1931>
- [6] Pavlenko N, Kopp T, Tsybmal EY, Mannhart J, Sawatzky GA (2012) Oxygen vacancies at titanate interfaces: two-

- dimensional magnetism and orbital reconstruction. *Phys Rev B* 86(6):064431. <https://doi.org/10.1103/PhysRevB.86.064431>
- [7] Pavlenko N, Kopp T, Tsymbal EY, Sawatzky GA, Mannhart J (2012) Magnetic and superconducting phases at the $\text{LaAlO}_3/\text{SrTiO}_3$ interface: the role of interfacial Ti 3d electrons. *Phys Rev B* 85(2):020407. <https://doi.org/10.1103/PhysRevB.85.020407>
- [8] Pavlenko N, Kopp T, Mannhart J (2013) Emerging magnetism and electronic phase separation at titanate interfaces. *Phys Rev B* 88(20):201104. <https://doi.org/10.1103/PhysRevB.88.201104>
- [9] Lechermann F, Boehnke L, Grieger D, Piefke C (2014) Electron correlation and magnetism at the $\text{LaAlO}_3/\text{SrTiO}_3$ interface: a DFT+DMFT investigation. *Phys Rev B* 90(8):085125. <https://doi.org/10.1038/ncomms5261>
- [10] Park J, Cho BG, Kim KD, Koo J, Jang H, Ko KT, Park JH, Lee KB, Kim JY, Lee DR, Burns CA, Seo SSA, Lee HN (2013) Oxygen-vacancy-induced orbital reconstruction of Ti ions at the interface of $\text{LaAlO}_3/\text{SrTiO}_3$ heterostructures: a resonant soft-X-ray scattering study. *Phys Rev Lett* 110(1):017401. <https://doi.org/10.1103/PhysRevLett.110.017401>
- [11] Salluzzo M, Gariglio S, Stornaiuolo D, Sessi V, Rusponi S, Piamonteze C, De Luca GM, Minola M, Marré D, Gadaleta A, Brune H, Nolting F, Brookes NB, Ghiringhelli G (2013) Origin of interface magnetism in $\text{BiMnO}_3/\text{SrTiO}_3$ and $\text{LaAlO}_3/\text{SrTiO}_3$ heterostructures. *Phys Rev Lett* 111(8):087204. <https://doi.org/10.1103/PhysRevLett.111.087204>
- [12] Piyanzina II, Eyert V, Lysogorskiy YV, Tayurskii DA, Kopp T (2019) Oxygen vacancies and hydrogen doping in $\text{LaAlO}_3/\text{SrTiO}_3$ heterostructures: electronic properties and impact on surface and interface reconstruction. *J Phys Condens Matter* 31(29):295601. <https://doi.org/10.1088/1361-648X/ab1831>
- [13] Burton JD, Tsymbal EY (2009) Prediction of electrically induced magnetic reconstruction at the manganite/ferroelectric interface. *Phys Rev B* 80(17):174406. <https://doi.org/10.1103/PhysRevB.80.174406>
- [14] Burton JD, Tsymbal EY (2012) Magnetoelectric interfaces and spin transport. *Philos Trans R Soc A Math Phys Eng Sci* 370(1977):4840–4855. <https://doi.org/10.1098/rsta.2012.0205>
- [15] Fang L, Aggoune W, Ren W, Draxl C. (2022) arXiv preprint [arXiv:2203.03881](https://arxiv.org/abs/2203.03881)
- [16] Cao C, Chen S, Deng J, Li G, Zhang Q, Gu L, Ying TP, Guo EJ, Guo JG, Chen X (2022) Two-dimensional electron gas with high mobility forming at $\text{BaO}/\text{SrTiO}_3$ interface. *Chin Phys Lett* 39(4):047301. <https://doi.org/10.1088/0256-307X/39/4/047301>
- [17] Chapman KS, Atkinson WA (2022) Mechanism for switchability in electron-doped ferroelectric interfaces. *Phys Rev B* 105(3):035307. <https://doi.org/10.1103/PhysRevB.105.035307>
- [18] Dong Y, Zhang L, Li C, Liu Y, Shao P, Lei J, Wang R, Wu D, Chen D, Zhang R, Zheng Y (2022) Stable pH sensitivity of $\text{LaAlO}_3/\text{SrTiO}_3$ interfacial electronic gas. *Curr Appl Phys* 34:55–58. <https://doi.org/10.1016/j.cap.2021.11.015>
- [19] Fredrickson KD, Demkov AA (2015) Switchable conductivity at the ferroelectric interface: nonpolar oxides. *Phys Rev B* 91(11):115126. <https://doi.org/10.1103/PhysRevB.91.115126>
- [20] Niranjana MK, Burton JD, Velev JP, Jaswal SS, Tsymbal EY (2009) Magnetoelectric effect at the $\text{SrRuO}_3/\text{BaTiO}_3$ (001) interface: an ab initio study. *Appl Phys Lett* 95(5):052501. <https://doi.org/10.1063/1.3193679>
- [21] Liu X, Tsymbal EY, Rabe KM (2018) Polarization-controlled modulation doping of a ferroelectric from first principles. *Phys Rev B* 97(9):094107. <https://doi.org/10.1103/PhysRevB.97.094107>
- [22] Duan CG, Jaswal SS, Tsymbal EY (2006) Predicted magnetoelectric effect in Fe/BaTiO_3 multilayers: ferroelectric control of magnetism. *Phys Rev Lett* 97(4):047201. <https://doi.org/10.1103/PhysRevLett.97.047201>
- [23] Yamauchi K, Sanyal B, Picozzi S (2007) Interface effects at a half-metal/ferroelectric junction. *Appl Phys Lett* 91(6):062506. <https://doi.org/10.1063/1.2767776>
- [24] Niranjana MK, Velev JP, Duan CG, Jaswal SS, Tsymbal EY (2008) Magnetoelectric effect at the $\text{Fe}_3\text{O}_4/\text{BaTiO}_3$ (001) interface: a first-principles study. *Phys Rev B* 78(10):104405. <https://doi.org/10.1103/PhysRevB.78.104405>
- [25] Cai T, Ju S, Lee J, Sai N, Demkov AA, Niu Q, Li Z, Shi J, Wang E (2009) Magnetoelectric coupling and electric control of magnetization in ferromagnet/ferroelectric/normal-metal superlattices. *Phys Rev B* 80(14):140415. <https://doi.org/10.1103/PhysRevB.80.140415>
- [26] Chen LY, Chen CL, Jin KX, Wu T (2014) Prediction of giant magnetoelectric effect in $\text{LaMnO}_3/\text{BaTiO}_3/\text{SrMnO}_3$ superlattice: the role of n-type $\text{SrMnO}_3/\text{LaMnO}_3$ interface. *J Appl Phys* 116(7):074102. <https://doi.org/10.1063/1.4893370>
- [27] Influences of orientation on magnetoelectric coupling at $\text{La}_{1-x}\text{Sr}_x\text{MnO}_3/\text{BaTiO}_3$ interface from Ab initio calculations. *J Electron Mater* 46(6):3808–3814. <https://doi.org/10.1007/s11664-016-5277-8>
- [28] Weng Y, Niu W, Huang X, An M, Dong S (2021) Ferroelectric control of a spin-polarized two-dimensional electron

- gas. *Phys Rev B* 103(21):214101. <https://doi.org/10.1103/PhysRevB.103.214101>
- [29] Spaldin NA, Ramesh R (2019) Advances in magnetoelectric multiferroics. *Nat Mater* 18(3):203–212. <https://doi.org/10.1038/s41563-018-0275-2>
- [30] Ederer C, Spaldin NA (2005) Recent progress in first-principles studies of magnetoelectric multiferroics. *Curr Opin Solid State Mater Sci* 9(3):128–139. <https://doi.org/10.1016/j.cossms.2006.03.001>
- [31] Nan CW, Bichurin MI, Dong S, Viehland D, Srinivasan G (2008) Multiferroic magnetoelectric composites: historical perspective, status, and future directions. *J Appl Phys* 103(3):031101. <https://doi.org/10.1063/1.2836410>
- [32] Fiebig M (2005) Revival of the magnetoelectric effect. *J Phys D Appl Phys* 38(8):R123. <https://doi.org/10.1088/0022-3727/38/8/R01>
- [33] Eerenstein W, Mathur ND, Scott JF (2006) Multiferroic and magnetoelectric materials. *Nature* 442(7104):759–765. <https://doi.org/10.1038/nature05023>
- [34] Ciucivara A, Sahu B, Kleinman L (2008) Density functional study of a ferromagnetic ferroelectric LaMnO₃/BaTiO₃ superlattice. *Phys Rev B* 77(9):092407. <https://doi.org/10.1103/PhysRevB.77.092407>
- [35] Kabanov VV, Piyanzina II, Lysogorskiy YV, Tayurskii DA, Mamin RF (2020) Ab initio investigation of electronic and magnetic properties of antiferromagnetic/ferroelectric LaMnO₃/BaTiO₃ interface. *Mater Res Express* 7(5):055020. <https://doi.org/10.1088/2053-1591/ab940e>
- [36] Hohenberg P, Kohn W (1964) Inhomogeneous electron gas. *Phys Rev* 136(3B):B864. <https://doi.org/10.1103/PhysRev.136.B864>
- [37] Kohn W, Sham LJ (1965) Self-consistent equations including exchange and correlation effects. *Phys Rev* 140(4A):A1133. <https://doi.org/10.1103/PhysRev.140.A1133>
- [38] Kresse G, Furthmüller J (1996) Efficiency of ab-initio total energy calculations for metals and semiconductors using a plane-wave basis set. *Comput Mater Sci* 6(1):5–50. [https://doi.org/10.1016/0927-0256\(96\)00008-0](https://doi.org/10.1016/0927-0256(96)00008-0)
- [39] Kresse G, Furthmüller J (1996) Efficient iterative schemes for ab initio total-energy calculations using a plane-wave basis set. *Phys Rev B* 54(16):11169. <https://doi.org/10.1103/PhysRevB.54.11169>
- [40] Kresse G, Joubert D (1999) From ultrasoft pseudopotentials to the projector augmented-wave method. *Phys Rev B* 59(3):1758. <https://doi.org/10.1103/PhysRevB.59.1758>
- [41] Medea version 3.4 (2022) Medea is a registered trademark of Materials Design, Inc., San Diego, USA
- [42] Electronic and magnetic properties of the BaTiO₃/LaMnO₃ interface: a DFT study. *J Supercond Novel Magn* 35:2225–2229. <https://doi.org/10.1007/s10948-022-06353-y>
- [43] Lines ME, Glass AM (2001) Principles and applications of ferroelectrics and related materials. Oxford University Press, Oxford
- [44] Janolin PE, Anokhin AS, Gui Z, Mukhortov VM, Golovko YI, Guiblin N, Ravy S, El Marssi M, Yuzyuk YI, Bellaiche L, Dkhil B (2014) Strain engineering of perovskite thin films using a single substrate. *J Phys Condens Matter* 26(29):292201. <https://doi.org/10.1088/0953-8984/26/29/292201>

Publisher's Note Springer Nature remains neutral with regard to jurisdictional claims in published maps and institutional affiliations.

Springer Nature or its licensor (e.g. a society or other partner) holds exclusive rights to this article under a publishing agreement with the author(s) or other rightsholder(s); author self-archiving of the accepted manuscript version of this article is solely governed by the terms of such publishing agreement and applicable law.